Feasibility and accuracy of multi-component models of ocean ambient noise to predict noise spectra on a short-time scale and assess long-term trends in noise components

Progress Report 2

Prepared by: Alexander Gavrilov

Centre for Marine Science and Technology

Prepared for: Office of Naval Research – Global

June 2021

This progress report summarizes the results of data analysis and modelling obtained within this project since August 2020.

The focus or research in the second year of the project was put on peculiarities of the underwater soundscape observed over the North West (NW) Shelf of Western Australia, in particular, in its northern part around and north of Scott Reef, which is of special research interest for the Defence Science and Technology Group (DSTG) in Australia. Empirical and numerical modelling efforts have been made to explain those peculiarities and improve the adequacy of prediction of underwater noise spectrum levels in this area.

The spectrum levels of wind-driven noise observed by long-term acoustic measurements at several sites in the northern part of the NW Shelf were noticeably lower than those predicted by the Cato's model (Cato, 1997) for wind-driven underwater noise suggested for the Australian continental shelf (Figure 1 (left panel) and Gavrilov *et al*., 2018, Gavrilov *et al*., 2020).

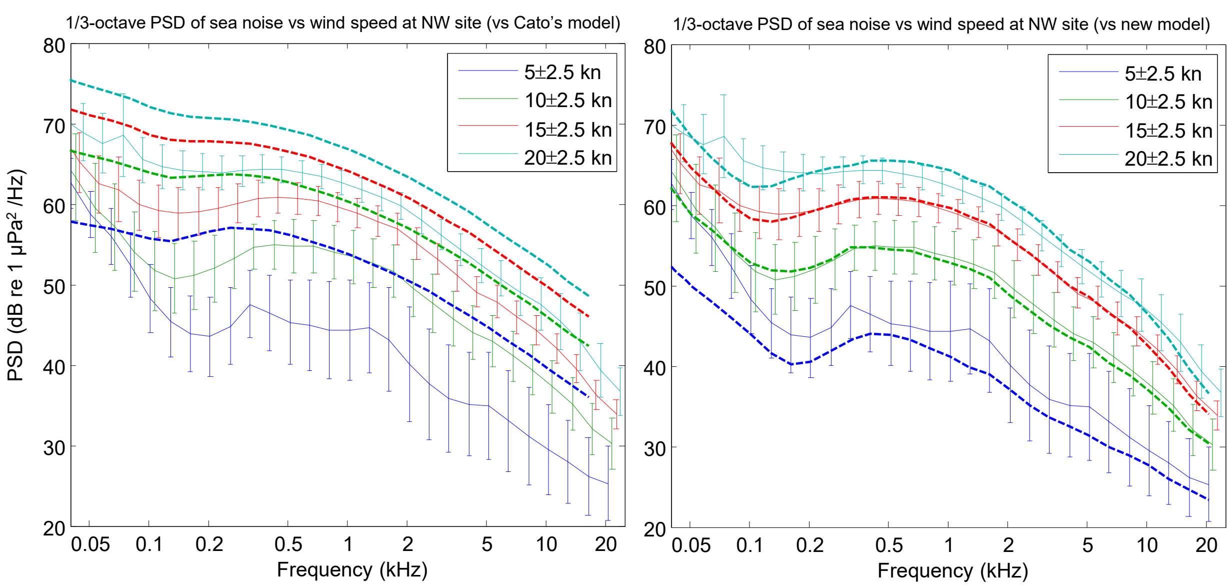

Figure1: Sea noise spectrum levels measured at one of the NW Shelf sites of acoustic measurements at different wind speeds (solid lines and error bars) and those predicted by the Cato's model of wind-driven noise spectrum levels in Australian waters (left panel, dashed lines) and by the new corrected empirical model (right panel, dashed lines).

The vertical directionality of wind-driven noise measured in the northern part of the NW Shelf was also atypical for the tropical and temperate ocean environments over continental shelves: the notch in the nearly horizontal direction of the vertical directionality pattern was missing with most of the sound energy arriving from the sea surface (Figure 2), although it was expected to be distinct at the critical angle $\varphi \approx 2 \cdot \cos^{-1}(C_a/C_s)$, where C_s is the sound speed at the sea surface and C_a is the sound speed at the array centre.

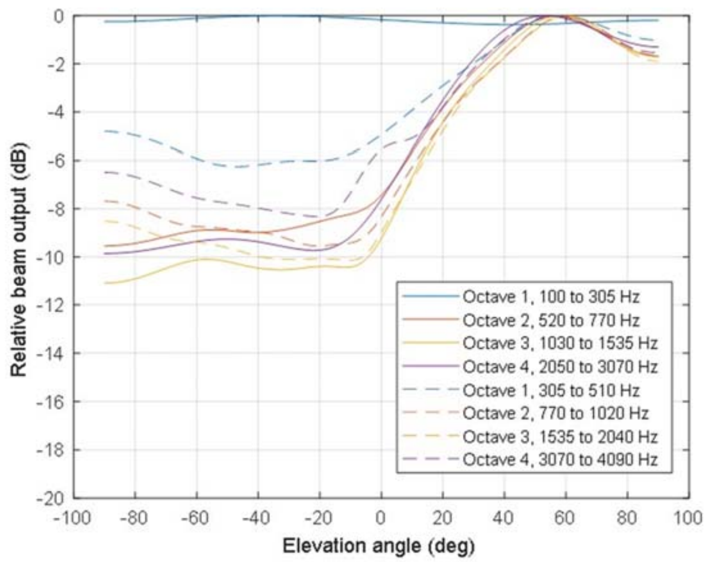

Figure 2: Beamformer outputs of a vertical array of ~38 m length, with the array centre placed at about 70 m below the sea surface, recording ocean ambient (primarily wind-driven) noise in the northern part of the NW Shelf. Notice that the beamforming results in the frequency band below 300 Hz (Octave 1) were corrupted by impulsive self-noise of the surface-mounted mooring system affected by wind waves.

The intensity of ship traffic over the northern part of the NW Shelf is significantly lower than that around the Perth Canyon and Portland sites of the Integrated Marine Observing System (IMOS, http://imos.org.au/facilities/nationalmooringnetwork/acousticobservatories/) considered in Year 1 of the project. Even if this fact is taken into consideration, the underwater noise levels from ships in the area of investigation is noticeably lower than that expected from the Automatic Identification System (AIS) data, a database of source spectrum levels of various ship types and an underwater sound propagation model (Gavrilov *et al*., 2018 and Gavrilov *et al*., 2019).

To explain the above-mentioned peculiarities of underwater noise observed in the northern part of the NW Shelf and build a model capable of predicting the ocean noise spectrum levels in the area of investigation, the following data analysis and modelling have been carried out:

1. Data on the sediment properties available from the area of interest have been hunted from various sources. Firstly, we found that core samples of sediments across the NW shelf were collected during an international oceanographic/geophysical survey Sonne 185 in 2005 (Kuhnt *et al.*, 2006). The core depth varied from about 8 m to nearly 16 m in the area of our interest. Most of the samples collected in the area between Scott and Ashmore reefs contained calcareous sand ("foraminiferal ooze") from the top to the bottom of cores.

   Data on sediment porosity and grain size were requested from Geoscience Australia (GA) for the study area. It appeared that the sediment porosity values just below the seabed interface were high, varying between 40% and 70%, and the median grain size values varied within 0.01-0.02 mm interval, which is typical for fine-to-medium silt.

2. Impulsive airgun noise from an offshore seismic survey (named Factory and conducted by Shell) was recorded at one of the acoustic monitoring sites in the study area between Scott and Ashmore reefs. The position of the survey vessel relative to the underwater sound recorder was known from AIS data, but parameters of the airgun array, used in the survey, were not. Analysis of received sound levels revealed that the noise level decayed with range to the noise source significantly faster than that observed in some other datasets of underwater sound recording that captured noise from offshore seismic exploration surveys over the Australian continental shelf.

Bearing the above-mentioned observations and facts in mind, a new model of underwater sound transmission loss was created and examined to explain the peculiarity of the soundscape in the study area. The model assumes highly porous sediments below the bottom interface overlaying a basement of much more consolidated sediment. Analysis of the head wave arrivals at different distances from the seismic source (Figure 3) suggests the thickness of the layer of unconsolidated or partly consolidated sediments to vary within 700±200 m and the compressional wave speed in the basement to be around 2600 m/s.

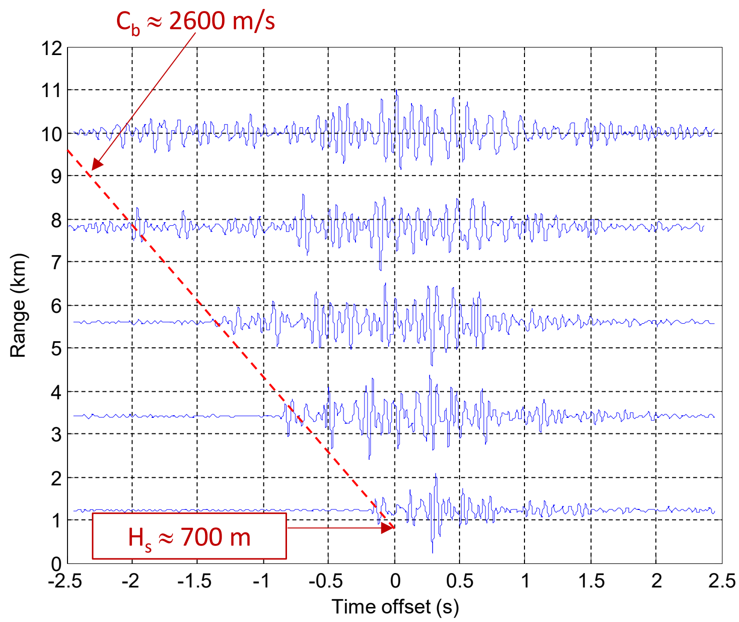

Figure 3: Waveform of low-pass filtered airgun signals received at the sound recorder at different distances from the sound source and aligned by the high-frequency waterborne arrivals. C_b is the sound speed in the basement and H_s is the sediment thickness above the basement, derived from the head wave arrivals.

Based on geological samples from boreholes and measurements of physical properties of calcareous sediments in the Indian Ocean (Bassinot *et al*., 1993, Alam, *et al*., 2010) and data presented in Bowless (1994 and 1997), the following geoacoustic model was examined in the attempt to numerically predict the sound transmission loss observed in the measurements of airgun signals from the offshore seismic survey:

1. In the top 700 m thick layer of unconsolidated ooze-like sediment and/or slightly consolidated chalk-like sediment, the porosity decreases linearly from 60% at the top to 45% at 700 mbs (meters below sea surface), which correspond to coefficient $\beta = 0.6$ and $\beta = 0.45$ respectively in the Biot's model (Biot, 1962) of sound velocity and attenuation in sediments.
2. An Effective Density Fluid Model (EDFM) from the Applied Physics Laboratory, UoW (Williams *et al*., 2002) was chosen for geoacoustic modelling, which is a slightly simplified version of the Biot's model. Parameters of the EDFM model are given in Table 1.
3. According to Bowless (1994), the shear wave (s-wave) velocity just below the seabed surface was assumed to be 120 m/s with a gradient of 0.2 s^{-1} from 0 to 700 mbs.
4. Using the results of head wave measurement, the compressional wave (p-wave) velocity in the underlying substrate was assumed to be 2600 m/s, which corresponds to either well consolidated limestone or claystone. Based on general properties of well consolidated sediments, the shear wave velocity was assumed to be 1200 m/s in the basement of the bottom model. The compressional and shear wave attenuation in the basement was assumed to be 0.3 and 0.6 dB/λ respectively.

Table 1: Parameters of the EDFM/Biot's model.

Depth	0 mbs	700 mbs
Water density ρ_W, kg/m^3	1023	1023
Sediment particle density ρ_S, kg/m^3	2690	2690
Sediment tortuosity α, dimensionless	1.35	1.35
Sediment porosity β, dimensionless	0.6	0.45
Sediment permeability κ, m^2	10^{-11}	10^{-11}
Water viscosity η, kg/(m·s)	0.001	0.001
Bulk modulus of sediment grains K_S, Pa	$3.2 \cdot 10^{10}$	$3.2 \cdot 10^{10}$
Bulk modulus of pore fluid (water) K_W, Pa	$2.395 \cdot 10^{9}$	$2.395 \cdot 10^{9}$

The dependence of p-wave velocity and attenuation on depth in the top layer and frequency calculated for the EDFM parameters given in Table 1 is shown in Figure 4.

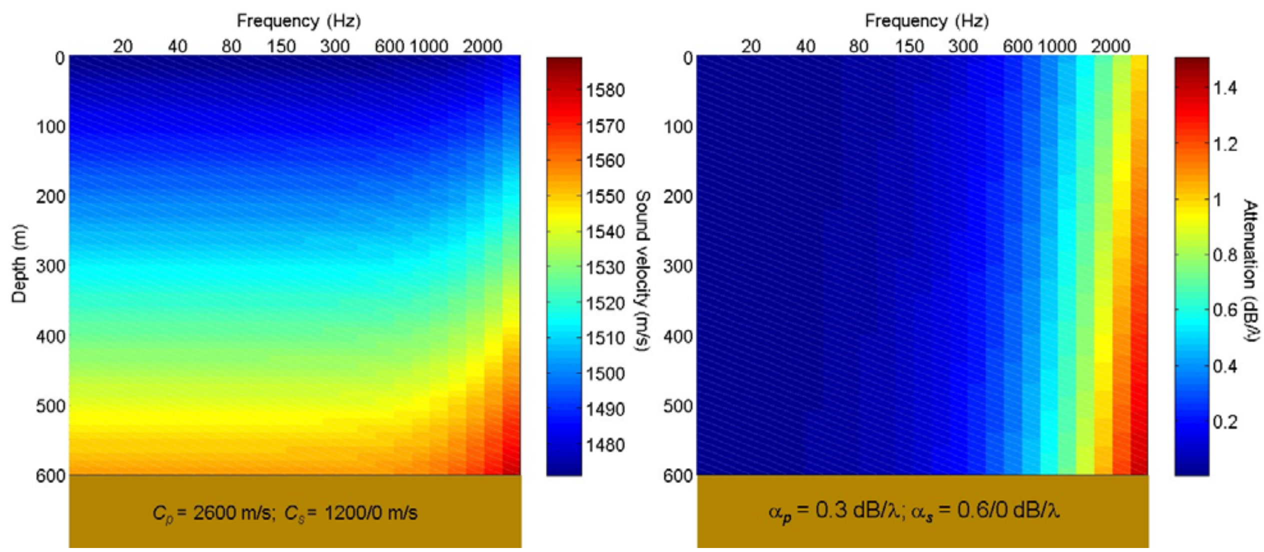

Figure 4: Dependence of compressional wave velocity (left) and attenuation (right) on depth and frequency calculated for the EDFM parameters given in Table 1.

The geoacoustic model of the seabed described above was used in the Wave Number Integration (WNI) underwater sound propagation model in a range independent environment, where the water depth and sound velocity profile (SVP) were taken at the location of sound recorder. These allowed us to consider the influence of shear in the sediments on the sound transmission loss (TL).

To make TL modelling possible for a range dependent ocean acoustic environment, the Parabolic Equation (PE) approximation model was also tested with the same geoacoustic model of the bottom, but no shear in it. To allow for considerably lower reflection from the ooze-limestone interface at low frequencies and small grazing angles due to the conversion of the incident p-wave energy into s-wave energy in the basement, the p-wave attenuation coefficient was deliberately increased to 10 dB/λ to simulate additional losses.

TL was modelled on a 1/3 octave frequency grid from 10 Hz to 2.6 kHz. It was averaged over each frequency band using the method described in Harrison and Harrison (1995). Then the mean sound level *I* measured in different frequency bands at ranges from 3 to 3.5 km was used as a reference value to estimate the source level in the corresponding band and then extrapolate numerical predictions of the sound level to larger ranges using the TL modelling results. The received sound levels resulting from modelling are compared to the measurements in Figure 5 for two selected frequency bands. In the other 1/3 octave bands, the trends are similar. At lower frequencies, the TL model tends to overestimate the sound energy loss compared to the measurement results, especially when shear in the top layer and basement is included in the model. As the sound frequency increases and the sound wavelength in the sediment becomes much smaller than the thickness of the top layer, the effect of shear in the basement reduces rapidly playing an insignificant role and the agreement between modelling and measurement results tends to be better. The role of shear in the top layer of unconsolidated sediments appears to be negligible.

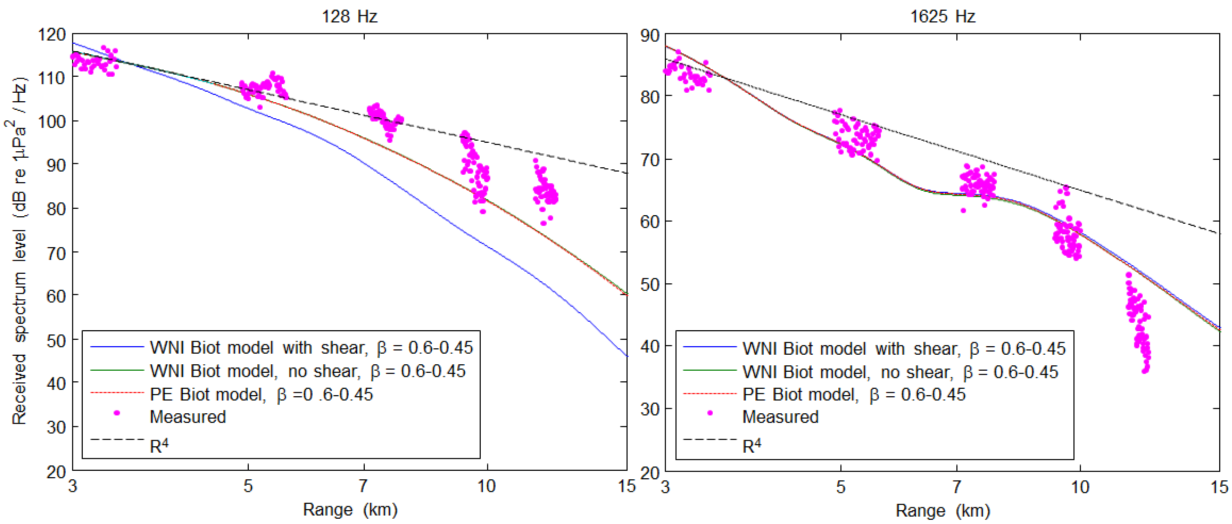

Figure 5: Measured (dots) and numerically modelled (solid lines) spectrum levels of airgun signals in two 1/3-octave bands centred at 128 Hz and ~1.6 kHz, received at different distances from the seismic source of the Factory survey transect. The black dashed line shows the sound energy decay of 40log(R).

The PE underwater sound propagation model with the suggested geoacoustic model of the seafloor was used to model the vertical directionality of wind-driven underwater noise and to examine the influence of bottom parameters on spectrum levels of wind-driven noise.

A point source of underwater noise was placed at 1 m below the sea surface to simulate an elementary source of wind noise, *i.e.* a cloud of collapsing air bubbles trapped in water by wind waves. Such an assumption regarding the source depth is most likely oversimplified, as the effective source depth of wind noise depends most likely on frequency; however, such dependence has not been thoroughly analysed and/or measured. A Green's function (GF) of the sound field was calculated over a distance of 50 km on a 10-m range grid and a depth grid of 0.2-m spacing spanning the entire water column.

Point sources of underwater noise were uniformly distributed over the modelled range of 50 km from the receiver location with the same 10-m spacing between sources. The source spectrum was assumed to be uniform with the source level of 0 dB re 1 μPa at 1. This is an unrealistic model of wind-driven noise, which is not suitable for modelling spectrum levels of wind noise; however, it is suitable for modelling its vertical directionality in relative units in each particular frequency band. The phases of sound waves from the point sources were uniformly randomly distributed on the full-circle interval of $(0, 2\pi)$, so that the sound of from different sources would be incoherent.

To calculate the resulting complex sound field at the receiver array, the contribution of all 5,000 incoherent sources was summed up and then vertical beamforming was applied to a vertical array of 3λ length with its centre placed at 70 m below the sea surface (λ is the sound wavelength in water). This operation was repeated 100,000 times for different realisations of random source phases to get more statistically reliable results by averaging.

Figure 6 shows the vertical directionality of the modelled wind noise in relative units versus frequency and elevation angle.

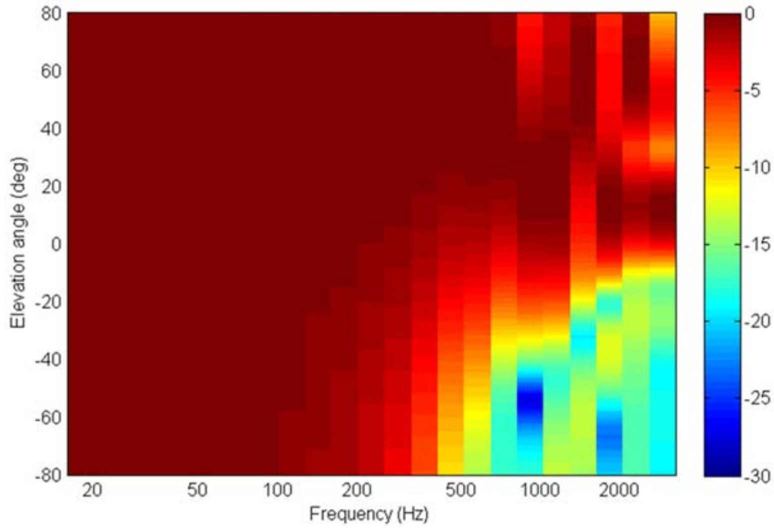

Figure 6: Vertical directionality of wind driven noise modelled at one of the NW Shelf sites at frequencies from 16 Hz to 2.6 kHz for the realistic downward refracting sound velocity profile and EDFM geoacoustic model of the seabed.

The modelling result does not fully agree with measurements (Figure 2) but is consistent in general. It also shows that most of the wind noise energy arrives from the sea surface and less is arriving from the bottom, although the difference between the surface generated and bottom reflected sound energy levels of 15-18 dB in the model is somewhat larger than 7-10 dB observed in the measurements.

Although the above-described model is not suitable for predicting spectrum levels of wind-driven noise, it still can be used to assess the influence of seafloor geoacoustic characteristics on noise levels. If we assume that the Cato's model is adequate for seabeds consisting of fine-to-medium sand, then we can calculate GF in the same way for a new bottom model and estimate the source spectrum level based on predictions from the Cato's model. Once this is done, it is possible to estimate spectrum levels of wind-driven noise for a bottom model of ooze-like sediment. To numerically simulate this, we assumed the porosity in sand-like sediment to vary from 30% at the seabed surface to 20% at the bottom of the top layer of unconsolidated sediment. This resulted in the sound speed increasing from about 1750 m/s to 1850 m/s, which corresponds to estimates for medium sand (Jensen *et al*., 2011). Then the GF numerical predictions for an ooze-like seabed were used along with the source spectrum level predictions to derive the spectrum level of wind-driven noise over the ooze-like sediment. Figure 7 compares the wind noise spectrum levels predicted from the Cato's model for three different wind speeds to those predicted for an ooze-like seabed, assuming the same source spectrum levels. The noise spectrum level predicted from the ooze-like seabed model is certainly lower than that predicted by the Cato's model, but the difference is noticeably smaller than that observed in the measurements on the NW Shelf, especially at low wind speeds (Figure 1, left panel).

Analysis of modelling results reveals that the contribution of remote wind-driven noise sources located beyond a couple of km from the receiver location was negligible compared to that from the near field, where the contribution of noise sources to the resulting noise level dominates. Figure 8 illustrates this finding.

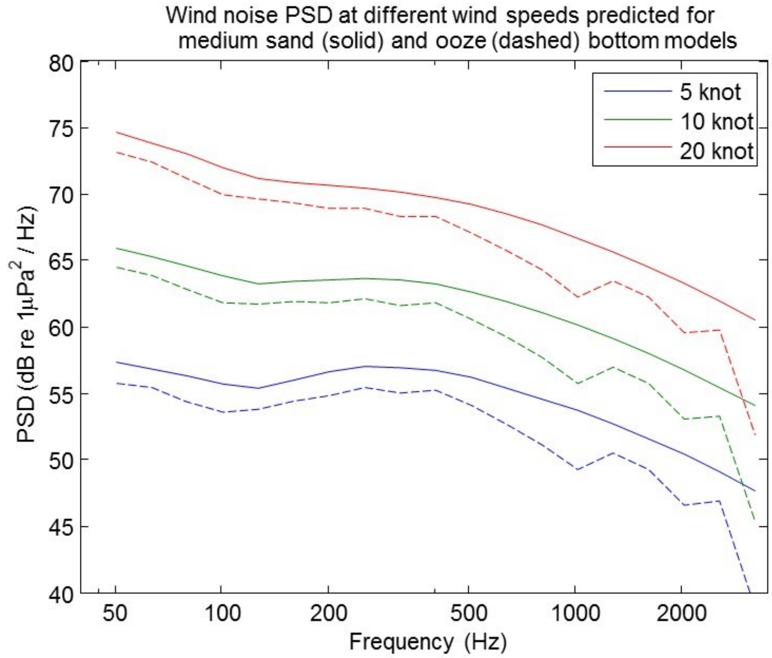

Figure 7: Spectrum levels of wind-driven underwater noise predicted by the Cato's model for different wind speeds (solid) and those numerically predicted for an ooze-like bottom.

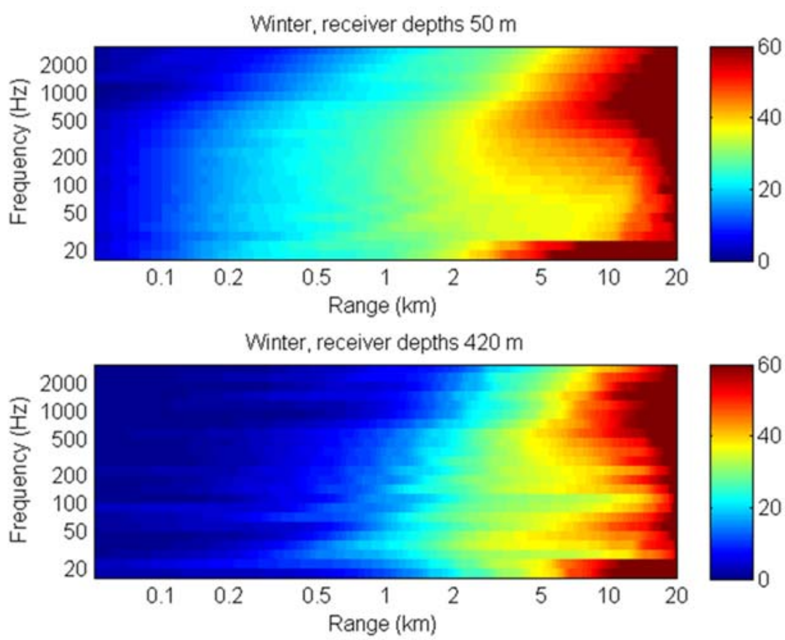

Figure 8: Modelled difference between the contribution of all near-surface sources of wind-driven noise within 20 km from the receiver to the total noise field and that from the cumulative contribution of remote sources located behind the range increasing in the x- axis of the plot.

Because the modelling approach described in the previous paragraphs did not result in a good agreement between the modelled and measured spectrum levels of wind-driven noise, an empirical method, similar to that used in the Cato's model, was employed.

An empirical model of spectrum level of wind-driven underwater noise in the study area was created using measurements of ocean noise at different wind speeds at a number of locations north of Scott

Reef. In the model, it is assumed that the dependence of wind noise spectrum level (NSL) can be approximated by NSL = $a + b \times \log(\textit{wind speed})$, where the wind speed is measured in knots. The coefficients a and b were derived from the best fit to the NSL measured at different wind speeds. As a result, the new empirical model of the spectrum level of wind noise fits the data collected in the study area in a much more satisfactory way than that predicted by the Cato's model (Figure 1, right panel); although the agreement of empirical modelling and measurement results is not perfect, especially for low wind speeds.

The geoacoustic model of the seabed, suggested and verified by a comparison of numerically predicted TL with the measurements of spectrum levels of impulsive airgun noise from the Factory offshore seismic survey, was used to model spectrum levels of ship noise and its statistics in the study area on the NW shelf. The modelling results show that the contribution ship noise to the ambient ocean noise field in the study area is negligible at least 75% of time. Moreover, the contribution of ship noise can be noticeable only at frequencies below approximately 80 Hz (Figure 9). Such statistics of ship noise differs significantly from the statistics and frequency band of ship noise observed in the other areas of the Australian shelf considered in this project, such as the Rottnest Island, Portland and NSW IMOS sites, where ship noise constitutes a significant and nearly permanent component of the underwater noise field, especially at low frequencies where cumulative contribution from distant shipping to the local noise field is noticeable. Moreover, at the IMOS acoustic sites, especially the NSW one, the events of nearby ship passage are much more frequent than that in the northern part of the NWS and the frequency band of ship noise during such events extends to higher frequencies up to 1 kHz and even higher.

In addition to the noticeably lower intensity of ship traffic over the northern part of the NW shelf, another key factor contributes to the reduction of ship noise, which is the low acoustic reflectivity of the seabed combined with strong downward sound refraction in this part of the Australian shelf.

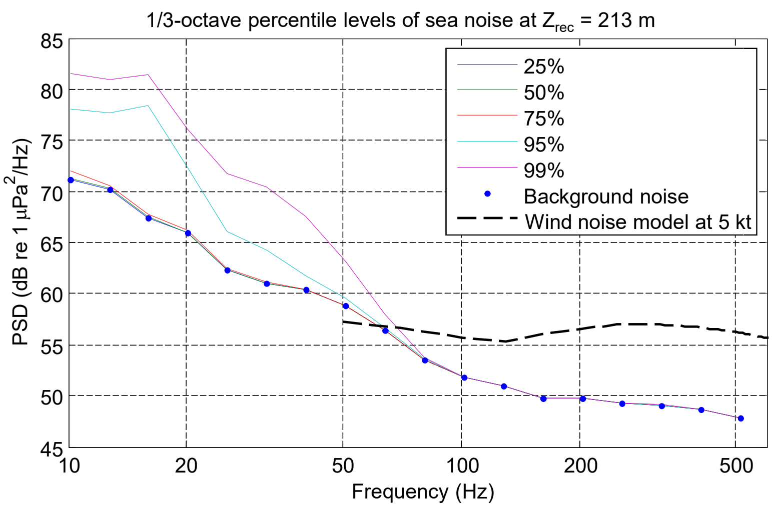

Figure 9: Statistics of spectrum levels of ship noise predicted by numerical modelling for the area northeast of Scott Reef for five different percentile values. Dots show the background spectrum level of underwater noise measured at wind speeds less than 5 knots and in the absence of other noise sources, such as whale calls, fish choruses, distant subsea earthquakes, etc. The dashed line shows prediction of wind noise spectrum level by the Cato's empirical model for wind speed of 5 knots.

References:

Alam, M.M., Borre, M.K., Fabricius, I.L. Hedegaard, K., Røgen, B., Hossain, Z., and Krogsbøll, A.S. (2010). "Biot's coefficient as an indicator of strength and porosity reduction: Calcareous sediments from Kerguelen Plateau", *J. Petrol. Sci. and Eng.* 70, 282–297.

Bassinot, F.C., Marsters, J.C., Mayer, L.A. and Wilkens, R.H. (1993). "Variations of porosity in calcareous sediments from the Ontong Java Plateau", *Proceedings of the Ocean Drilling Program, Scientific Results,* Vol. 130, pp.653-661.

Biot, M.A. (1962), "Generalized theory of acoustic propagation in porous dissipative media," *J. Acoust. Soc. Amer.* 34(5), 1254–1264.

Bowles, F.A. (1994). "A Geoacoustic Model for Fine-Grained, Unconsolidated Calcareous Sediments (ARSRP Natural Laboratory)", NRL Report 94-10451

Bowles, F.A. (1997). "Observations on attenuation and shear-wave velocity in fine-grained, marine sediments", *J. Acous. Soc. Am.* 101(6), 3385-3397.

Cato, D.H., "Ambient sea noise in Australian waters", in *Proc. of 5th International Congress on Sound and Vibration, International Institute of Acoustics and Vibration*, p. 2813 (1997).

Gavrilov, A.N., McCauley, R.M. and Zhang, Z.Y. (2018a). "Composite model of ocean ambient noise in the Perth Canyon area", CMST Report 2018-05 prepared for DSTG, Curtin University, 2018.

Gavrilov, A.N., McCauley, R.M. and Zhang, Z.Y. (2018b). "Models of Wind and Rain Driven Underwater Noise", CMST Report 2018-02 prepared for DSTG, Curtin University, 2018.

Gavrilov, A.N., McCauley, R.M. and Zhang, Z.Y. (2019). "Feasibility and accuracy of prediction of ocean noise on a short-time scale", in *Proc. of Underwater Acoustic Conference and Exhibition*, Crete 2019, pp. 375-382.

Gavrilov, A.N., McCauley, R.M., Jenner, C. and Zhang, Z.Y. (2020). "Analysis of long-term and in-situ measurement data of ocean ambient noise collected over the northern part of the North West Shelf of Australia in 2019-2020 and modelling of ocean noise based on experimental measurements", CMST Report 2020-18 prepared for DSTG, Curtin University, 2020.

Harrison, C.H. and Harrison, J.A. (1996). "A simple relationship between frequency and range averages for broadband sonar", *J. Acoust. Soc. Am.* 97(2), 1314-1317.

Jensen, F.B., Kuperman, F.A., Porter, M A., and Schmidt, H. (2011). *Computational Ocean Acoustics*, 2nd ed., New York, NY, USA, Springer-Verlag.

Kuhnt, W., *et al*. (2005). "Variability of the Indonesian Throughflow and Australasian climate history of the last 150,000 years", VITAL Cruise Report SONNE 185, Darwin – Jakarta, 15 September 2005 – 6 October 2005 (https://www.tib.eu/en/suchen/id/awi:doi~10.2312%252Fcr_so185/).

Mears, C. A., Scott, J., Wentz, F. J., Ricciardulli, L., Leidner, S. M., Hoffman, R., and Atlas, R. (2019). "A Near-Real-Time Version of the Cross-Calibrated Multiplatform (CCMP) Ocean Surface Wind Velocity Data Set", *Journal of Geophysical Research: Oceans* 124, 6997 – 7010.

Williams, K.L., Jackson, D.R., Thorsos, E.I., Tang, D. and Schock, S.G. (2002). "Comparison of Sound Speed and Attenuation Measured in a Sandy Sediment to Predictions Based on the Biot Theory of Porous Media", *IEEE J. Ocean. Eng*. 27(3), 413-428.